# Charged-current quasielastic (anti)neutrino cross sections on $^{12}$C with realistic spectral functions including meson-exchange contributions

M. V. Ivanov, A. N. Antonov, G. D. Megias, J. A. Caballero, M. B. Barbaro, J. E. Amaro, I. Ruiz Simo, T. W. Donnelly, and J. M. Udías

View Online          Export Citation

**ARTICLES YOU MAY BE INTERESTED IN**

Relativistic models for electron and neutrino-nucleus scattering
AIP Conference Proceedings **1189**, 107 (2009); https://doi.org/10.1063/1.3274139

Superscaling analyses of inclusive electron scattering and their extension to charge-changing neutrino cross sections in nuclei
AIP Conference Proceedings **899**, 3 (2007); https://doi.org/10.1063/1.2733028

Charged-current inclusive neutrino cross sections in the SuperScaling model
AIP Conference Proceedings **1722**, 030005 (2016); https://doi.org/10.1063/1.4944128

# Charged-Current Quasielastic (Anti)Neutrino Cross Sections on $^{12}$C with Realistic Spectral Functions Including Meson-Exchange Contributions

M.V. Ivanov[1,a)], A.N. Antonov[1], G.D. Megias[2], J.A. Caballero[2], M.B. Barbaro[3], J.E. Amaro[4], I. Ruiz Simo[4], T.W. Donnelly[5] and J.M. Udías[6]

[1]*Institute for Nuclear Research and Nuclear Energy, Bulgarian Academy of Sciences, Sofia 1784, Bulgaria*
[2]*Departamento de Física Atómica, Molecular y Nuclear, Universidad de Sevilla, 41080 Sevilla, Spain*
[3]*Dipartimento di Fisica, Università di Torino and INFN, Sezione di Torino, Via P. Giuria 1, 10125 Torino, Italy*
[4]*Departamento de Física Atómica, Molecular y Nuclear, and Instituto de Física Teórica y Computacional Carlos I, Universidad de Granada, Granada 18071, Spain*
[5]*Center for Theoretical Physics, Laboratory for Nuclear Science and Department of Physics, Massachusetts Institute of Technology, Cambridge, Massachusetts 02139, USA*
[6]*Grupo de Física Nuclear, Departamento de Estructura de la Materia, Física Aplicada y Electrónica and UPARCOS, Universidad Complutense de Madrid, CEI Moncloa, 28040 Madrid, Spain*

a)Corresponding author: martin@inrne.bas.bg

**Abstract.** We present a detailed study of charged-current quasielastic (anti)neutrino scattering cross sections on a $^{12}$C target obtained using a spectral function $S(p, \mathcal{E})$ that gives a scaling function in accordance with the electron scattering data. The spectral function accounts for the nucleon-nucleon ($NN$) correlations, it has a realistic energy dependence and natural orbitals (NO's) from the Jastrow correlation method are used in its construction. The results are compared with those when $NN$ correlations are not included, namely harmonic-oscillator single-particle wave functions are used instead of NO's. A comparison of the results with recent experiments, as well as to results from the superscaling approach is done. The contribution of two-particle two-hole meson-exchange currents on neutrino–nucleus interactions is also considered within a fully relativistic Fermi gas. The results show a good agreement with the experimental data over the whole range of neutrino energies.

## INTRODUCTION

The study of charged-current mediated quasi-elastic (CCQE) neutrino-nucleus scattering in the GeV region is a powerful tool for hadronic and nuclear studies. We note that although in the tradition of neutrino experiments the term 'elastic', either charged-current elastic or neutral-current elastic is used for neutrino scattering off free nucleons as well as on nucleons bound on nuclei, in this work we will refer to the latter case with the more precise denomination of quasi-elastic (QE). Recently, the MiniBooNE [1, 2] and Miner$\nu$a [3, 4] collaborations have produced high-quality data, using a mostly carbon target, for a number of selected channels, in particular, for the Quasi-Elastic (QE) one, that is, where no pions are detected in the final state. The treatment of nuclear effects represents one of the main sources of systematic uncertainty in the experimental determination of neutrino oscillation parameters. In particular, the CCQE MiniBooNE results [1, 2] have stimulated many theoretical studies devoted to explaining the apparent discrepancies between data and most theoretical predictions based on the impulse approximation (IA). Based on results from different groups, the inclusion of effects beyond IA, such as multinucleon excitations, mainly two-particle two-hole meson-exchange current (2p-2h MEC) contributions, has allowed one to explain these data without including any effective parameter (such as the axial mass $M_A$) [5–9].

The aim of the present paper is to continue our work from Ref. [10] using the results obtained in Ref. [11] for a realistic spectral function $S(p, \mathcal{E})$ instead of the phenomenological superscaling approximation (SuSA) approach. The spectral function from our previous work [10] will be applied to analysis of CCQE (anti)neutrino cross sections

on a $^{12}$C target measured by the MiniBooNE [1, 2] and Miner$\nu$a [3, 4] experiments. The new aspect of the present calculation concerns the treatment of 2p-2h excitations. In this work we include the fully relativistic weak (with vector and axial components) charged meson-exchange currents, in both longitudinal and transverse channels. These have been evaluated in Refs. [12–14] from an exact microscopic calculation, where the two-body current is the sum of seagull, pion-in-flight, pion-pole, and $\Delta$-pole operators and the basis wave functions are noninteracting Dirac spinors.

## GENERAL FORMALISM

### Expression for the Cross Sections

We consider the process where an incident beam of (anti)neutrinos with 4-momentum $K^\mu = (\epsilon, \mathbf{k})$ scatters off a nuclear target and a charged lepton with 4-momentum $K'^\mu = (\epsilon', \mathbf{k}')$ emerges. The 4-momentum transfer $Q^\mu = (\omega, \mathbf{q}) \equiv (\epsilon - \epsilon', \mathbf{k} - \mathbf{k}')$ is spacelike: $-Q^2 = q^2 - \omega^2 > 0$. The CC (anti)neutrino-nucleus inclusive cross section in the target laboratory frame can be written in the form (see Refs. [15, 16] for details)

$$\left[ \frac{d^2\sigma}{d\Omega dk'} \right]_\chi = \sigma_0 \mathcal{F}_\chi^2, \tag{1}$$

where $\chi = +$ for neutrino-induced reactions (in the QE case, $\nu_\ell + n \rightarrow \ell^- + p$, where $\ell = e, \mu, \tau$) and $\chi = -$ for antineutrino-induced reactions (in the QE case, $\bar{\nu}_\ell + p \rightarrow \ell^+ + n$). The function $\mathcal{F}_\chi^2$ in Eq. (1) depends on the nuclear structure and is presented as a generalized Rosenbluth decomposition [15] containing leptonic kinematical factors, $V_K$, and five nuclear response functions, $R_K$, namely $VV$ and $AA$ charge-charge ($CC$), charge-longitudinal ($CL$), longitudinal-longitudinal ($LL$) and transverse ($T$) contributions, and $VA$ transverse ($T'$) contributions, where $V(A)$ denotes vector(axial-vector) current matrix elements. These are specific components of the nuclear tensor $W^{\mu\nu}$ in the QE region and can be expressed in terms of the superscaling function $f(\psi)$ (see Ref. [15] for explicit expressions).

## Models: HO+FSI, NO+FSI, and SuSAv2

In the mentioned experiments the interaction of the neutrino occurs with nucleons bound in nuclei. The analyses of such processes within different methods involve various effects such as nucleon-nucleon ($NN$) correlations, the final state interactions (FSI), possible modifications of the nucleon properties inside the nuclear medium and others. These effects, however, cannot be presently accounted for in an unambiguous and precise way, and what is very important, in most cases they are highly model-dependent. A possible way to avoid the model-dependencies is to use the nuclear response to other leptonic probes, such as electrons, under similar conditions to the neutrino experiments. The superscaling approximation (SuSA) follows this general trend. The analyses of superscaling phenomena observed in electron scattering on nuclei have led to the use of the scaling function directly extracted from $(e, e')$ data to predict (anti)neutrino-nucleus cross sections [15], just avoiding the usage of a particular nuclear structure model. A "superscaling function" $f(\psi)$ has been extracted from the data by factoring out the single-nucleon content of the double-differential cross section and plotting the remaining nuclear response versus a scaling variable $\psi(q, \omega)$ ($q$ and $\omega$ being the momentum transfer and transferred energy, respectively). For high enough values of the momentum transfer (roughly $q > 400$ MeV/c) the explicit dependence of $f(\psi)$ on $q$ is very weak at transferred energies below the quasielastic peak (scaling of the first kind). Scaling of second kind (*i.e.* no dependence of $f(\psi)$ on the mass number $A$) turns out to be excellent in the same region. The term "superscaling" means the occurrence of both first and second types of scaling.

In this work we consider three different theoretical calculations. Two of them, denoted as HO (harmonic oscillator) and NO (natural orbitals), make use of a spectral function $S(p, \mathcal{E})$, $p$ being the momentum of the bound nucleon and $\mathcal{E}$ the excitation energy of the residual nucleus, coinciding with the missing energy $E_m$ up to a constant offset [17]. The area of analyses of the scaling function, the spectral function, and their connection (see, *e.g.*, Refs. [11, 18]) provides insight into the validity of the mean-field approximation (MFA) and the role of the $NN$ correlations, as well as into the effects of FSI. Though in the MFA it is possible, in principle, to obtain the contributions of different shells to $S(p, \mathcal{E})$ and $n(p)$ for each single-particle state, owing to the residual interactions the hole states are not eigenstates of the residual nucleus but are mixtures of several single-particle states. The latter leads to the spreading of the shell structure and requires studies of the spectral function using theoretical methods going beyond the MFA to describe successfully the relevant experiments. In Ref. [11] a realistic spectral function $S(p, \mathcal{E})$ has been constructed that is in
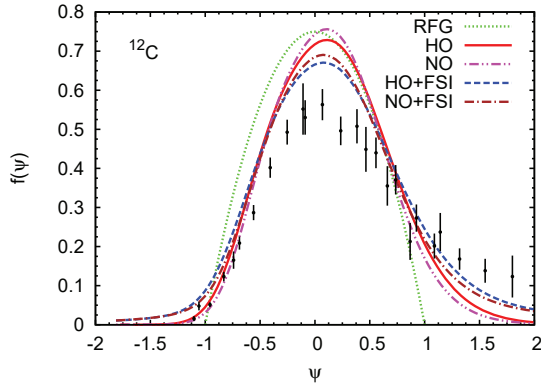
**FIGURE 1.** (Color online) Results for the superscaling function $f(\psi)$ for $^{12}$C obtained using HO and NO approaches with (HO+FSI and NO+FSI) and without FSI (HO and NO) are compared with the RFG results, as well as with the longitudinal experimental data.
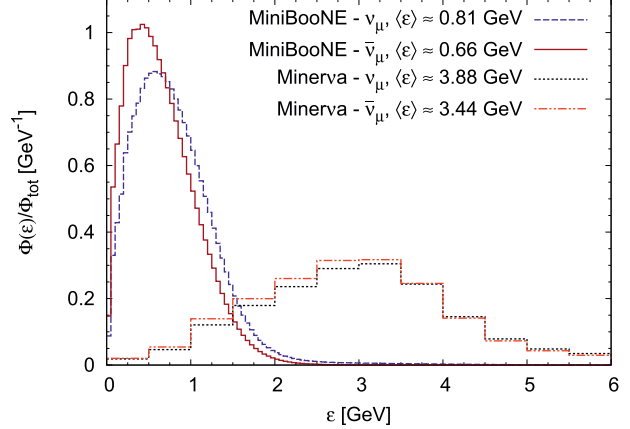


**FIGURE 2.** (Color online) The predicted $\nu_\mu$ ($\bar{\nu}_\mu$) fluxes at the MiniBooNE [26] and MINER$\nu$A [27] detectors and corresponding mean energies.

agreement with the scaling function $f(\psi)$ obtained from the $(e, e')$ data. For this purpose effects beyond MFA have been considered. The procedure included (i) the account for effects of a finite energy spread and (ii) the account for *NN* correlation effects considering single-particle momentum distributions $n_i(p)$ [that are components of $S(p, \mathcal{E})$] beyond the MFA, such as those related to the usage of natural orbitals (NO's) [19] for the single-particle wave functions and occupation numbers within methods in which short-range *NN* correlations are included. For the latter the Jastrow correlation method [20] has been considered. Also, in Ref. [11] FSI were accounted for using complex optical potential that has given a spectral function $S(p, \mathcal{E})$, leading to asymmetric scaling function in accordance with the experimental analysis, thus showing the essential role of the FSI in the description of electron scattering reactions.

In Fig. 1 the results for the superscaling function $f(\psi)$ within the HO+FSI and NO+FSI models [10, 11] are presented. As a reference also shown are the superscaling functions obtained without FSI and in the RFG model, as well as the longitudinal experimental data [15]. Accounting for FSI leads to a redistribution of the strength, with lower values of the scaling function at the maximum and an asymmetric shape around the peak position, *viz.,* when $\psi = 0$. The two spectral function models, including FSI, clearly give a much more realistic representation of the data than the relativistic Fermi gas.

The third model, SuSAv2, is an improved version of the superscaling prescription, called SuSAv2 [21], has been developed by incorporating relativistic mean field (RMF) effects [22–24] in the longitudinal and transverse nuclear responses, as well as in the isovector and isoscalar channels. This is of great interest in order to describe CC neutrino reactions that are purely isovector. Note that in this approach the enhancement of the transverse nuclear response emerges naturally from the RMF theory as a genuine relativistic effect.

The detailed description of the SuSAv2 model can be found in Refs. [9, 21, 25]. Here we just mention that it has been validated against all existing $(e, e')$ data sets on $^{12}$C, yielding excellent agreement over the full range of kinematics spanned by experiments, except for the very low energy and momentum transfers, where all approaches based on impulse approximation (IA) are bound to fail. Furthermore, the success of the model depends on the inclusion of effects associated with two-body electroweak currents, which will be briefly discussed in the next Section.

## 2p-2h MEC Contributions

Ingredients beyond the impulse approximation (IA), namely 2p-2h MEC effects, are essential in order to explain the neutrino-nucleus cross sections of interest for neutrino oscillation experiments [6–9, 28, 29]. In particular, 2p-2h MEC effects produce an important contribution in the "dip" region between the QE and $\Delta$ peaks, giving rise to a significant enhancement of the impulse approximation responses in the case of inclusive electron- and neutrino-nucleus scattering processes. In this work we make use of the 2p-2h MEC model developed in Ref. [13], which is an extension to the weak sector of the seminal papers [30–32] for the electromagnetic case. The calculation is entirely based on the RFG

model, and it incorporates the explicit evaluation of the five response function involved in inclusive neutrino scattering. The MEC model includes one-pion-exchange diagrams derived from the weak pion production model of Ref. [33]. This is at variance with the various scaling approaches that are largely based on electron scattering phenomenology, although also inspired in some cases by the RMF predictions.

Following previous works [9, 25, 34, 35], here we make use of a general parametrization of the MEC responses that significantly reduces the computational time. Its functional form for the cases of $^{12}$C and $^{16}$O is given in Refs. [9, 25, 36], and its validity has been clearly substantiated by comparing its predictions with the complete relativistic calculation. The main merit of this procedure is that it can easily be incorporated into the Monte Carlo neutrino event generators used in the analysis of neutrino oscillation experiments.

## ANALYSIS OF RESULTS

In this section we show the predictions of the two spectral function approaches previously described, HO and NO, both including FSI and 2p–2h MEC. We compare the results with data from different experiments: MiniBooNE and MINERvA. Our study is restricted to the QE-like regime where the impulse approximation in addition to the effects linked to the 2p-2h meson-exchange currents play the major role. We follow closely the general analysis presented in Ref. [9] for the case of the superscaling approach. Hence, for reference, we compare our new theoretical predictions with the results corresponding to the SuSAv2-MEC model.

The predicted $\nu_\mu$ and $\bar{\nu}_\mu$ fluxes at the MiniBooNE [26] and MINERvA [27] detectors and corresponding mean energies are compared in Fig. 2. $\Phi_{\text{tot}}$ is the total integrated $\nu_\mu$ ($\bar{\nu}_\mu$) flux factor: $\Phi_{\text{tot}} = \int \Phi(\epsilon)d\epsilon$, where $\epsilon$ is incident beam energy. The neutrino and antineutrino mean energies corresponding to MiniBooNE experiment are around 0.8 and 0.7 GeV, whereas the MINERvA energy flux is much more extended to higher energies, with an average value close to $3.5 - 4.0$ GeV.

## MiniBooNE

In Figs. 3 and 4 we show the double differential cross section averaged over the neutrino and antineutrino energy flux against the kinetic energy of the final muon. The data are taken from the MiniBooNE Collaboration [1, 2]. We represent a large variety of kinematical situations where each panel refers to results averaged over a particular muon angular bin.
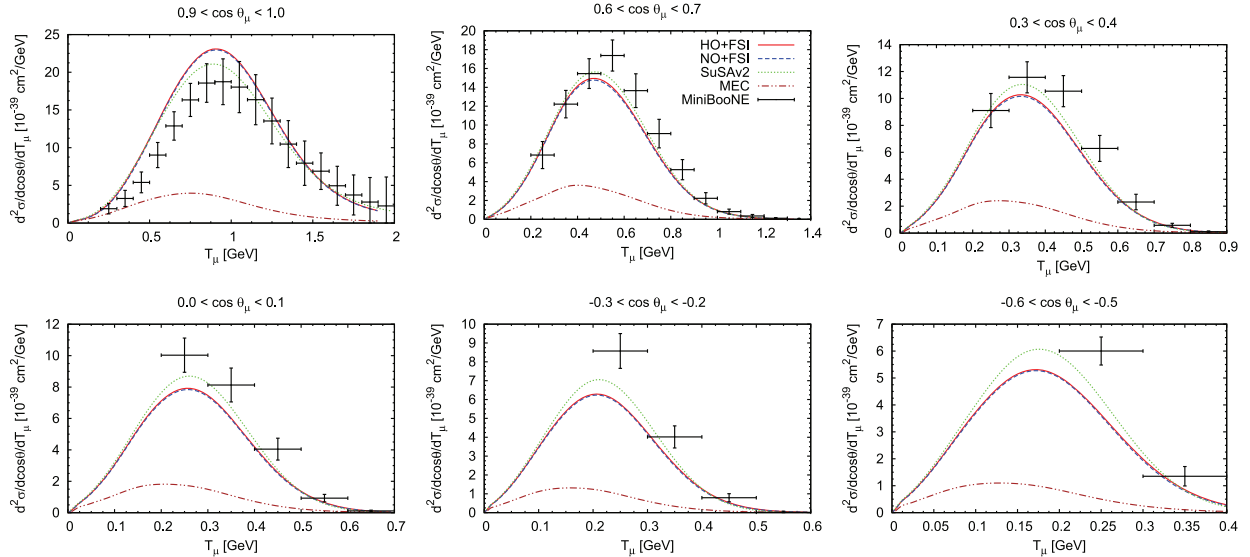


**FIGURE 3.** (Color online) MiniBooNE flux-folded double differential cross section per target neutron for the $\nu_\mu$ CCQE process on $^{12}$C displayed versus the $\mu^-$ kinetic energy $T_\mu$ for various bins of $\cos\theta_\mu$ obtained within the SuSAv2, HO+FSI, and NO+FSI approaches including MEC. 2p–2h MEC results are shown separately. The data are from Ref. [1].
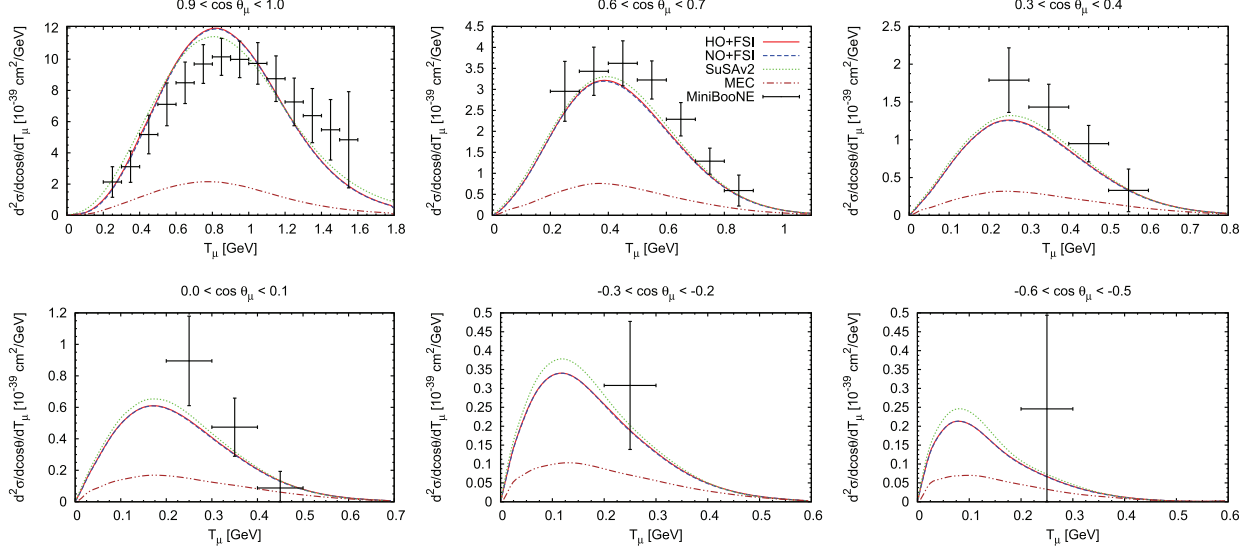
**FIGURE 4.** (Color online) As for Fig. 3, but now for the $\bar{\nu}_\mu$ CCQE process on $^{12}$C. The data are from Ref. [2].

We compare the data with the results obtained within the HO+FSI, NO+FSI, and SuSAv2 approaches, all of them including 2p–2h MEC, that are also presented separately. As already shown in Ref. [9], notice the relevant role played by 2p-2h MEC contributions, of the order of ~20-25% of the total response at the maximum. In the neutrino case (Fig. 3) this relative strength is almost independent of the scattering angle, except for the most forward bin, $0.9 < \cos\theta_\mu < 1$, where the MEC contribution is ~15%; this angular bin, however, largely corresponds to very low excitation energies ($\omega < 50$ MeV) and in this case completely different modeling, appropriate for the near-threshold regime, should be used. In the antineutrino case (Figs. 4) the 2p-2h relative strength gets larger for backward scattering angles ($\cos\theta_\mu < -0.2$). This is due to the fact that the antineutrino cross section involves a destructive interference between the $T$ and $T'$ channels and is therefore more sensitive to nuclear effects.

Theoretical predictions including both the QE and the 2p-2h MEC contributions are in good accord with the data in most of the kinematical situations explored. Only at scattering angles approaching 90° and above does one see a hint of a difference, although in these situations only a small number of data points with large uncertainties exist.

With regard to the comparison between the different models, we observe that HO+FSI and NO+FSI provide almost identical responses in all kinematical situations for neutrinos and antineutrinos: the inclusive cross section is not sensitive to the details of the spectral function. Compared with SuSAv2, some differences emerge whose magnitude depends on the scattering angle region explored. Whereas the SuSAv2 prediction is slightly smaller than the SF+FSI one at very forward kinematics (very small energy and momentum transfers), the reverse tends to occur as $\theta_\mu$ gets larger. Notice that at the most backward kinematics for neutrinos, the SuSAv2 results exceed by ~15% those of the SF+FSI model at the maximum. Similar comments also apply to antineutrinos (Fig. 4).

## MINERνA

The results in Fig. 5 correspond to the MINERνA flux averaged CCQE $\nu_\mu(\bar{\nu}_\mu)$ differential cross section per nucleon as a function of the reconstructed four-momentum $Q^2_{\rm QE}$, that is obtained in the same way as for the experiment, assuming an initial state nucleon at rest with a constant binding energy, $E_b$, set to 34 MeV (30 MeV) in the neutrino (antineutrino) case. The left panel refers to $\nu_\mu$–$^{12}$C (a), whereas the right panel contains predictions and data for $\bar{\nu}_\mu$–CH (b).

As shown, the spread in results ascribed to the three models used is minimal, of the order of ~1% − 2%. On the other hand, we note the excellent agreement between the theory and data once 2p-2h MEC effects (~20% − 30% of the total) are included. This significant contribution of the 2p-2h MEC effects is consistent with the results observed for MiniBooNE in spite of the very different muon neutrino (antineutrino) energy fluxes in the two experiments.
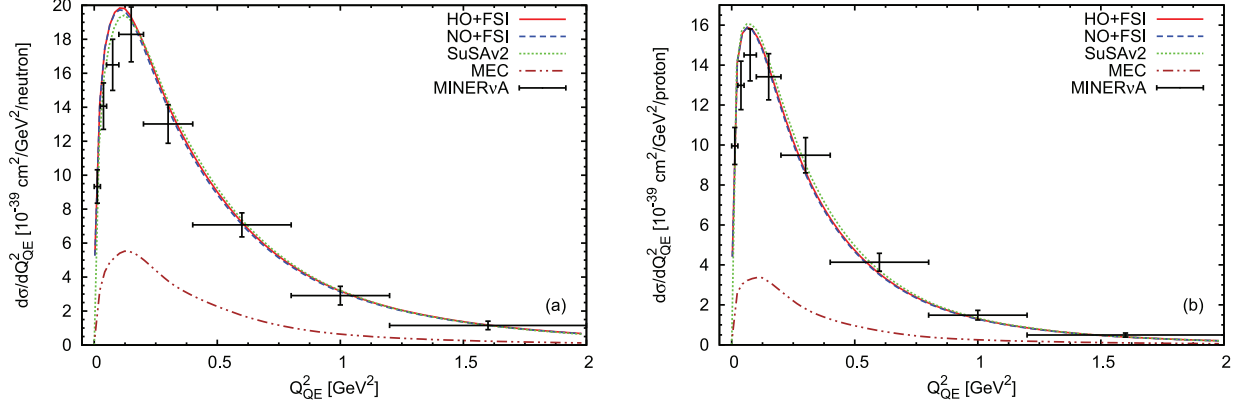
**FIGURE 5.** (Color online) Flux-folded CCQE $\nu_\mu$–$^{12}$C (a) and $\bar{\nu}_\mu$–CH (b) scattering cross section per target nucleon as a function of $Q^2_{\rm QE}$ and evaluated in the SuSAv2, HO+FSI, and NO+FSI approaches including MEC. The MINER$\nu$A data are from Ref. [3, 4].

## CONCLUSIONS

This work extends our previous studies of CCQE neutrino-nucleus scattering processes that are of interest for neutrino (antineutrino) oscillation experiments. Here we focus on models based on the use of two spectral functions, one of them including *NN* short-range correlations through the Jastrow method and, for a comparison, another without them. Effects of final-state interactions are also incorporated by using an optical potential. These calculations, based on the impulse approximation, are complemented with the contributions given by two-body weak meson exchange currents, giving rise to two-particle two-hole excitations. The model is applied to two different experiments, MiniBooNE and MINER$\nu$A.

These new predictions are compared with the systematic analysis presented in Ref. [9] based on the SuSAv2-MEC approach. We find that the spectral function based models (HO+FSI, NO+FSI) lead to results that are very close to the SuSAv2-MEC predictions. Only at the most forward and most backward angles do the differences become larger, being at most of the order of $\sim 10\% - 12\%$. This is in contrast with the contribution ascribed to the 2p-2h MEC effects that can be even larger than $\sim 30\% - 35\%$ compared with the pure QE responses. This proves without ambiguity the essential role played by 2p-2h MEC in providing a successful description of neutrino (antineutrino)-nucleus scattering data for different experiments and a very wide range of kinematical situations.

An interesting outcome of the present study is that the results obtained with the NO spectral function, which accounts for *NN* short-range Jastrow correlations, are almost identical to those obtained with the uncorrelated HO spectral function, thus indicating that the role played by this type of correlations is very minor for the observables analyzed in this study. The results in this work can be seen as a test of the reliability of the present spectral function based models. They compare extremely well with the SuSAv2 approach, based on the phenomenology of electron scattering data, although they fail in reproducing neutrino (antineutrino) scattering data unless ingredients beyond the impulse approximation are incorporated. The present study gives us confidence in extending the use of these models to other processes, such as semi-inclusive CC$\nu$ reactions and neutral current processes.

## ACKNOWLEDGMENTS

# REFERENCES

[1] A. A. Aguilar-Arevalo *et al.* (MiniBooNE Collaboration), Phys. Rev. D **81**, p. 092005 (2010).

[2] A. A. Aguilar-Arevalo *et al.* (MiniBooNE Collaboration), Phys. Rev. D **88**, p. 032001 (2013).

[3] G. A. Fiorentini *et al.* (MINERvA Collaboration), Phys. Rev. Lett. **111**, p. 022502 (2013), the values come from a private communication, MINERvA collaboration.

[4] L. Fields *et al.* (MINERvA Collaboration), Phys. Rev. Lett. **111**, p. 022501 (2013), the values come from a private communication, MINERvA collaboration.

[5] M. Martini, M. Ericson, G. Chanfray, and J. Marteau, Phys. Rev. C **80**, p. 065501 (2009).

[6] J. E. Amaro *et al.*, Phys. Lett. B **696**, 151–155 (2011).

[7] J. Nieves, I. Ruiz Simo, and M. J. Vicente Vacas, Physics Letters B **707**, 72 – 75 (2012).

[8] O. Lalakulich, K. Gallmeister, and U. Mosel, Phys. Rev. C **86**, p. 014614 (2012).

[9] G. D. Megias *et al.*, Phys. Rev. D **94**, p. 093004 (2016).

[10] M. V. Ivanov *et al.*, Phys. Rev. C **89**, p. 014607 (2014).

[11] A. N. Antonov *et al.*, Phys. Rev. C **83**, p. 045504 (2011).

[12] I. R. Simo *et al.*, Phys. Rev. D **90**, p. 033012 (2014).

[13] I. Ruiz Simo *et al.*, J. Phys. **G44**, p. 065105 (2017).

[14] I. R. Simo *et al.*, Phys. Rev. C **94**, p. 054610 (2016).

[15] J. E. Amaro *et al.*, Phys. Rev. C **71**, p. 015501 (2005).

[16] D. B. Day, J. S. McCarthy, T. W. Donnelly, and I. Sick, Annu. Rev. Nucl. Part. Sci. **40**, 357–410 (1990).

[17] M. Barbaro, R. Cenni, A. D. Pace, T. Donnelly, and A. Molinari, Nuclear Physics A **643**, 137 – 160 (1998).

[18] J. A. Caballero *et al.*, Phys. Rev. C **81**, p. 055502 (2010).

[19] P.-O. Löwdin, Phys. Rev. **97**, 1474–1489 (1955).

[20] M. V. Stoitsov, A. N. Antonov, and S. S. Dimitrova, Phys. Rev. C **48**, 74–86 (1993).

[21] R. González-Jiménez *et al.*, Phys. Rev. C **90**, p. 035501 (2014).

[22] J. A. Caballero *et al.*, Phys. Rev. Lett. **95**, p. 252502 (2005).

[23] J. A. Caballero, Phys. Rev. C **74**, p. 015502 (2006).

[24] J. Caballero, J. Amaro, M. Barbaro, T. Donnelly, and J. Udías, Physics Letters B **653**, 366 – 372 (2007).

[25] G. D. Megias *et al.*, Phys. Rev. D **94**, p. 013012 (2016).

[26] A. A. Aguilar-Arevalo *et al.* (MiniBooNE Collaboration), Phys. Rev. D **79**, p. 072002 (2009).

[27] L. Aliaga *et al.* (MINERvA Collaboration), Phys. Rev. D **94**, p. 092005 (2016).

[28] T. Katori and M. Martini, Journal of Physics G: Nuclear and Particle Physics **45**, p. 013001 (2018).

[29] L. Alvarez-Ruso *et al.*, Prog. Part. Nucl. Phys. **100**, 1–68 (2018).

[30] J. W. Van Orden and T. W. Donnelly, Annals Phys. **131**, 451–493 (1981).

[31] A. De Pace, M. Nardi, W. M. Alberico, T. W. Donnelly, and A. Molinari, Nucl. Phys. **A726**, 303–326 (2003).

[32] J. E. Amaro *et al.*, Phys. Rev. C **82**, p. 044601 (2010).

[33] E. Hernández, J. Nieves, and M. Valverde, Phys. Rev. D **76**, p. 033005 (2007).

[34] G. D. Megias *et al.*, Phys. Rev. D **91**, p. 073004 (2015).

[35] M. V. Ivanov *et al.*, Journal of Physics G: Nuclear and Particle Physics **43**, p. 045101 (2016).

[36] G. D. Megias *et al.*, (2017), arXiv:1711.00771 [nucl-th] .